Thermal deformation measurement of electronic packages using the atomic force microscope scanning moiré technique

Y. G. Lu,[a] Z. W. Zhong, and J. Yu
Precision Engineering and Nanotechnology Centre, School of Mechanical and Production Engineering, Nanyang Technological University, Nanyang Avenue, Singapore 639798

H. M. Xie
Sensor and Actuator Strategic Research Program, School of Mechanical and Production Engineering, Nanyang Technological University, Nanyang Avenue, Singapore 639798

B. K. A. Ngoi
Precision Engineering and Nanotechnology Centre, School of Mechanical and Production Engineering, Nanyang Technological University, Nanyang Avenue, Singapore 639798

G. B. Chai and A. Asundi
Sensor and Actuator Strategic Research Program, School of Mechanical and Production Engineering, Nanyang Technological University, Nanyang Avenue, Singapore 639798

(Received 26 September 2000; accepted for publication 2 January 2001)

In this article, the feasibility of atomic force microscope (AFM) scanning moiré on a cross-line diffraction grating has been studied. The AFM scanning moiré technique has been applied to measure the thermal deformation of electronic packages successfully. This technique is convenient to perform the mismatch method, also it could obtain a higher resolution than any other moiré method. © *2001 American Institute of Physics.* [DOI: 10.1063/1.1350641]

I. INTRODUCTION

Electronic packaging is the technology dealing with the protection of a silicon chip from the environment, as well as both electrical and mechanical connections to the surrounding components. The package contains various conducting or insulating materials that have different coefficients of thermal expansion (CTE); these differences of CTE lead to thermally induced mechanical stresses within the package when the package is powered on. As the components and structures in electronic packages become smaller and more complicated, the thermal gradient may increase and the strain concentration becomes more serious.

The moiré technique is a whole field *in situ* method to measure the in-plane deformation. Its excellent abilities, such as high displacement measurement sensitivity, high spatial resolution, and high signal-to-noise ratio, made it ideal for measuring complex geometry. Han has made a thorough review of this technique and its application to deformation measurement in microelectronic devices.[1]

The scanning probe microscope (SPM) was developed in the 1980s for its high spatial resolution. It has found many applications in a broad range of fields, including microelectronics. As one of the most popular members of SPM family, the atomic force microscope (AFM) has been used extensively to perform dimensional measurements such as Z dimensions, roughness, and critical dimensions in the semiconductor industry where the sizes of circuit elements are steadily shrinking.[2] The AFM moiré technique was also developed to measure deformation in a very small scale as compared with microscopic moiré interferometries. Chen, Liu, and Lee demonstrated the feasibility of using AFM to form moiré fringe patterns.[3] The AFM scanning lines were used as the reference grating and the specimen grating could be prepared by various methods. Xie *et al.* had successfully applied the AFM moiré technique to measure nanodeformation of mica and high-orientated pyrolytic graphite (HOPG) in which the atomic lattice of mica and HOPG was used as the specimen grating.[4]

In this article, the AFM moiré technique was applied to measure the thermal deformation of quad flat pack (QFP) packages. The AFM scanning lines were used as the reference grating and a diffraction grating attached to the specimen was used as the specimen grating. The results have proven that AFM moiré is a suitable technique for such applications.

II. AFM MOIRÉ ON DIFFRACTION GRATING

The AFM measurement principle is well known since it is now widely used. The probing tip at the end of a cantilever scans and collects data in a raster pattern. A constant force, either van der Waals or Coulombic, keeps the cantilever deflected at a preset amplitude. A laser beam is focused on the cantilever and is reflected to a photodiode detector array, effectively measuring the height of the cantilever. This height information is then transferred back to the controller as a feedback signal to adjust the voltage applied to a piezotube so that the force between the scanning tip and sample features is constant. By recording the voltage applied to the piezotube, the topography of a sample can be mapped.

While topography measurement is common knowledge, the raster movement pattern of the scanner is similar to the

[a]Author to whom correspondence should be addressed; electronic mail: p146704367@ntu.edu.sg

 © 2001 American Institute of Physics
Reuse of AIP Publishing content is subject to the terms at: https://publishing.aip.org/authors/rights-and-permissions. Download to IP: 155.69.24.171 On: Sat, 03 Sep 2016 08:32:32

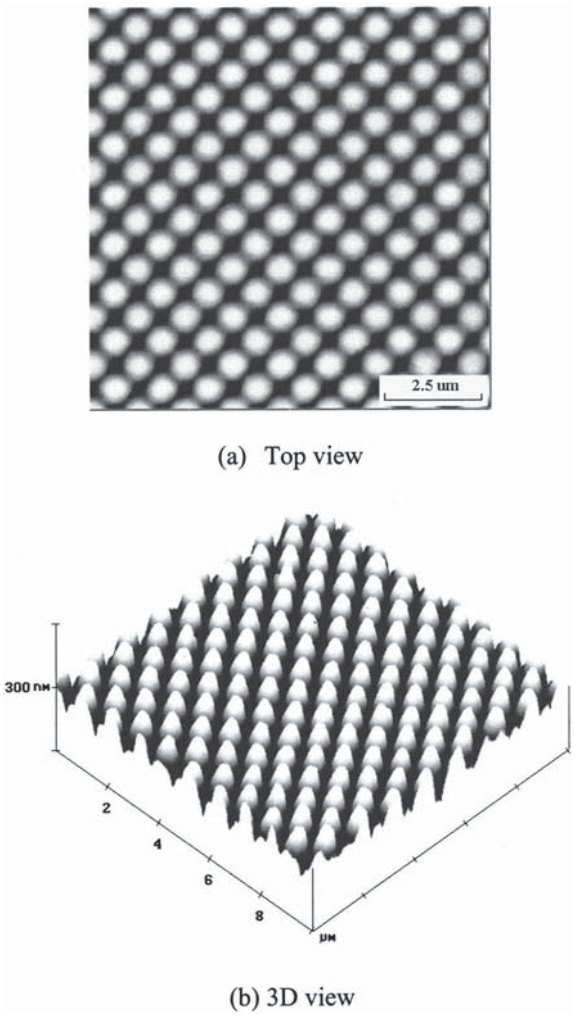

FIG. 1. AFM image of the cross-line diffraction grating (1200 lines/mm).

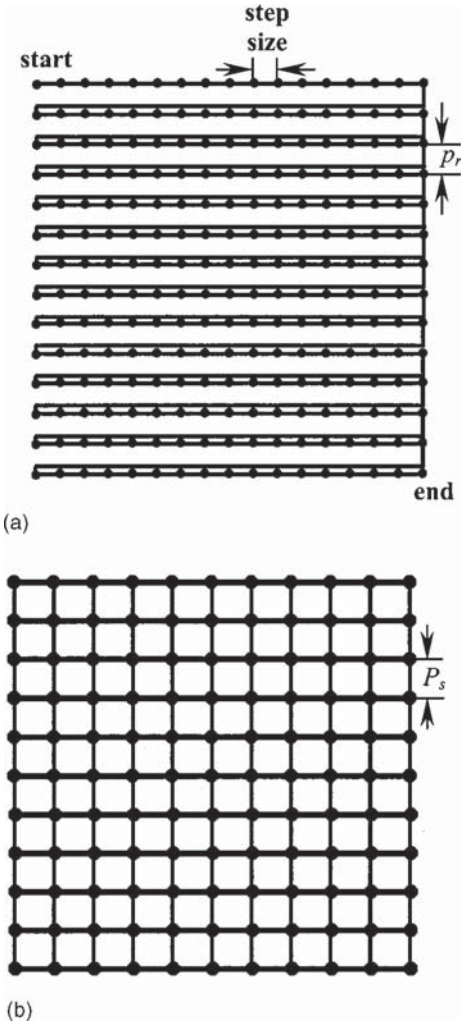

FIG. 2. Schematic diagram of reference and specimen gratings. (a) Raster pattern motion of AFM scanner. (b) Schematic diagram of diffraction grating.

scanning lines of a TV camera in the scanning moiré proposed by Morimoto and Hayashi[5] in the early 1980s. The scanning movement of the AFM scanner can also be taken as a parallel grating to form the scanning moiré. When the scanning lines were taken as the reference grating, they may interfere with a matching specimen grating to generate scanning moiré fringes.

The AFM moiré technique is novel compared with traditional moiré technologies, false moiré fringes may emerge due to several unidentified factors. For new specimen gratings, the feasibility of forming moiré fringes should be confirmed before the measurements are carried out.

The feasibility of AFM moiré has been shown using a scanning electron microscope generated parallel grating,[3] mica, and a HOPG lattice.[4] However, in traditional moiré techniques, diffraction grating is much more popular. Figure 1 shows the topography of a standard cross-line 1200 lines/mm diffraction grating. In this study, this grating was tested to form AFM moiré fringes. Uniformity of this grating was examined by AFM and its error was within 0.5%.

The reference and specimen grating are schematically illustrated in Fig. 2. The AFM scanner scans and collects data in a raster pattern, as shown in Fig. 2(a), the scanning lines can be taken as the reference grating while the diffraction grating is taken as the specimen grating. AFM moiré fringes were formed by the overlapping of the two gratings, as shown in Fig. 3.

In order to verify that the captured fringes are really interfered with by the specimen grating and reference grating, the scanning lines were rotated slightly with respect to the specimen grating since moiré fringes should also rotate following Eq. (1):[6]

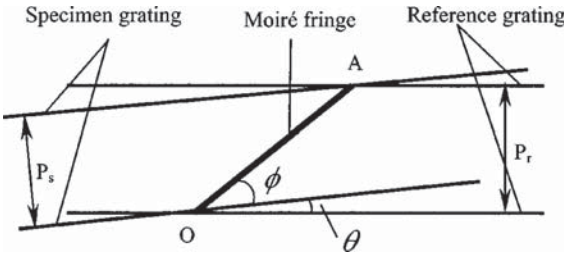

FIG. 3. Schematic diagram of moiré fringe formation.

Reuse of AIP Publishing content is subject to the terms at: https://publishing.aip.org/authors/rights-and-permissions. Download to IP: 155.69.24.171 On: Sat, 03 Sep 2016 08:32:32

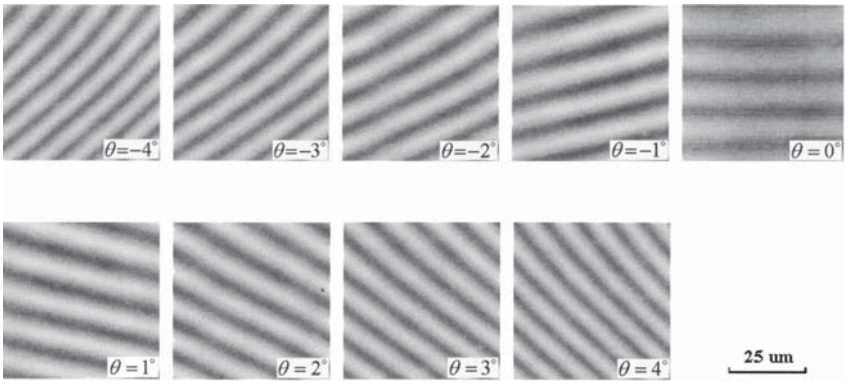

FIG. 4. Moiré fringe patterns at various scan angles.

$$\frac{\sin(\phi-\theta)}{\sin\phi}=\frac{p_s}{p_r}=C, \tag{1}$$

where ϕ and θ are the moiré fringe rotation angle and specimen grating rotation angle with respect to the reference grating, i.e., scanning lines, respectively; p_s and p_r are pitch values of the specimen grating and reference grating, respectively, as shown in Fig. 3. In this feasibility test, all images were captured by using 128 scanning lines in a 100 μm scanning range. Hence, $p_r=100/128=0.78125\,\mu$m, $p_s=1000/1200=0.83333\,\mu$m, and $C=p_s/p_r=1.0667$.

For convenience of verifying experimental and analytical results, the specimen grating was carefully aligned so that the grating was parallel to the 0° scan angle of the scanner. Then, the scan angle was changed from −4° to 4° with a step of 1°. AFM moiré fringes were captured with a 100 μm scan size, as shown in Fig. 4. The maximum scan size kept dropping as the scan angle increased, otherwise more images at various angles could have been captured.

Table I shows the analytical and experimental results of the AFM moiré test; the experimental results coincide well with the analytical values.

Another verification method is to change the frequency of the reference grating when θ is kept fixed. Adjusting the AFM scan size changed the reference grating frequency. When θ was 0°, the interfringe spacing varied with the changes of the scan size. The experimental results also coincide well with those of theoretical analysis.

The conclusion can be made that the moiré fringes are really AFM moiré fringes formed by the specimen and reference grating and can be applied to the deformation measurement.

TABLE I. Analytical and experimental results of moiré fringe angles.

θ	ϕ_T [a]	ϕ_E [b]
−4	45.27	44.57
−3	37.57	37.19
−2	27.42	27.38
−1	14.64	14.55
0	0	0
1	−14.64	−14.88
2	−27.42	−28.45
3	−37.57	−37.65
4	−45.27	−44.68

[a] ϕ_T : theoretical analysis results.
[b] ϕ_E : experimental results.

III. STRAIN MEASUREMENT BY USING THE AFM MOIRÉ TECHNIQUE

The frequency of the reference grating depends on the scan size L and number of scanning lines N. Because AFM scanners usually cannot scan a size beyond 150 μm, and there are only several options for the number of scanning lines (64, 128, 256, 512), attention should be paid to choose a proper scan size.

Supposing that in a scan size of L there are two fringes, then the frequency of reference grating can be taken as[4]

$$f_r=\frac{1}{p_r}=\frac{N}{L}\quad (N=64,\,128,\,256,\,512), \tag{2}$$

where N is the number of scanning lines. And the strain can be defined as

$$\varepsilon_y=\frac{|p_s-p_r|}{p_r}=\frac{p_s}{L}. \tag{3}$$

From Eqs. (2) and (3) the scan size can be defined as

$$L=p_s(N\mp 1). \tag{4}$$

Similarly, when in the scanned area there are l orders of moiré fringes, the strain ε_y can be defined as

$$\varepsilon_y=\frac{|p_s-p_r|}{p_r}=\frac{l-1}{L}p_s. \tag{5}$$

From Eqs. (2) and (5), the scan size can be determined as

$$L=p_s[N\mp(l-1)]. \tag{6}$$

From Eq. (6), a null field could be obtained for an ideal reference grating and specimen grating if the scan size and number of scan lines were carefully chosen. However, due to imperfection of reference and specimen gratings and in some cases the need to eliminate the strain induced by other factors such as temperature variation, a virtual strain is usually required for better measurement accuracy. For example, instead of using a 107 μm scan size to produce a null field, a 100 μm scan size could produce a desired number of moiré fringes before deformation.

Reuse of AIP Publishing content is subject to the terms at: https://publishing.aip.org/authors/rights-and-permissions. Download to IP: 155.69.24.171 On: Sat, 03 Sep 2016 08:32:32

When the carrier moiré was used to measure the in-plane deformation, the virtual normal strain in the y direction can be measured as

$$\varepsilon_y^0=\frac{\partial v_y^0}{\partial y}=\frac{p_s}{S_{yy}^0}, \tag{7}$$

where the U and V fields are the moiré pattern in the x and y directions, and S_{yy}^0 is the spacing between the two adjacent fringes in the V-field initial moiré pattern.

After exerting a load and using the same scan size and number of scan lines in the initial moiré pattern, the normal strain in the y direction can be measured as

$$\varepsilon_y^1=\frac{\partial v_y^1}{\partial y}=\frac{p_s}{S_{yy}^1}, \tag{8}$$

where v_y^1, ε_y^1 are the displacement and normal strain in the y direction after deformation, respectively. S_{yy}^1 is the spacing between two adjacent fringes corresponding to the deformed V-field moiré pattern.

Strain introduced by the load can be determined as

$$\varepsilon_y=\varepsilon_y^1-\varepsilon_y^0=\frac{\partial v_y^1}{\partial y}-\frac{\partial v_y^0}{\partial y}=\frac{p_s}{S_{yy}^1}-\frac{p_s}{S_{yy}^0}. \tag{9}$$

In this study, the cross-line diffraction grating was taken as two identical parallel gratings orthogonal to each other (as shown in Figs. 1 and 2). By simply rotating the scan angle to 90°, the U-field moiré pattern could record similarly, and the normal strain in the x direction can be measured as

$$\varepsilon_x=\varepsilon_x^1-\varepsilon_x^0=\frac{\partial u_x^1}{\partial x}-\frac{\partial u_x^0}{\partial x}=\frac{p_s}{S_{xx}^1}-\frac{p_s}{S_{xx}^0}, \tag{10}$$

then the shear strain can be determined as

$$\gamma_{xy}=\frac{\partial u^1}{\partial y}+\frac{\partial v^1}{\partial x}-\frac{\partial u^0}{\partial y}-\frac{\partial v^0}{\partial x}=\frac{p_s}{S_{xy}^1}+\frac{p_s}{S_{yx}^1}-\frac{p_s}{S_{xy}^0}-\frac{p_s}{S_{yx}^0}, \tag{11}$$

where u^0 and u^1 are the displacement components in the x direction before and after deformation, respectively; S_{xy}^0 is the spacing between the adjacent U-field moiré fringe in the y direction before deformation, S_{yx}^0 is the spacing between the adjacent V-field moiré fringes in the x direction before deformation, and S_{xy}^1 and S_{yx}^1 are the spacing between the adjacent U and V fields in the y and x directions, respectively.

The sign of normal strain can be determined by rotating the scan angle. When the moiré fringes rotate in the same direction, the normal strain is tensile; otherwise, it is compressive. Note that in this study, the AFM rotates in the clockwise direction when the scan angle increases.

IV. AFM MOIRÉ APPLICATION TO ELECTRONIC PACKAGES

In this study, a quad flat pack package was cleaved in half to expose the internal components and then polished flat to a fineness 0.02 level to attach a diffraction grating. Figure 5 schematically shows the cross section of the QFP package.

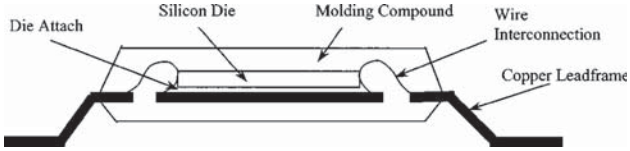

FIG. 5. Schematic diagram of QFP (the package contains various materials that have different CTE).

The cross-line diffraction grating (shown in Fig. 1) with a frequency of 1200 lines/mm was heated with the package, and the grating was made on an ultra-low-expansion substrate so that it will not change with temperature. Both the package and the grating were kept at the elevated temperature long enough to ensure the same temperature and proper relaxation. Then, the grating was transferred to the ground surface at 100 °C and cooled down to 25 °C immediately. The specimen was thus subjected to an isothermal loading of $\Delta T=-75\,^{\circ}\mathrm{C}$. The grating deformed with the specimen during the cool-down process.

The deformed package was carefully mounted onto the AFM stage using adhesive plastic, with its longer sides parallel to the y axis of the stage, as shown in Fig. 6. Due to the symmetry of the package deformation, adjustments were carefully made to find the neutral point O located approximately at the center of the cross section. This was done when uniform parallel moiré fringes were observed with a 0° scan angle, as shown in Fig. 7.

One of the most interesting areas where cracks tend to initiate was the corner of the silicon die. Six points along the y axis just out of the die attach to the corner were observed, both U- and V-field moiré images were captured. Examples are shown in Figs. 8 and 9.

Using Eqs. (3)–(11), the normal strain and shear strain can be calculated.

Figure 10 shows the distribution of normal strain dV/dy values at the die corner. It can be seen that this normal strain decreases gradually while the corner experienced the highest

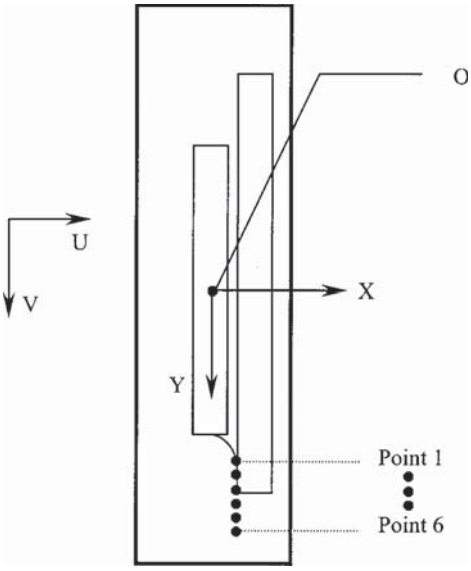

FIG. 6. Schematic diagram of specimen orientation (the specimen was mounted parallel to the y axis to find the neutral point).

Reuse of AIP Publishing content is subject to the terms at: https://publishing.aip.org/authors/rights-and-permissions. Download to IP: 155.69.24.171 On: Sat, 03 Sep 2016 08:32:32

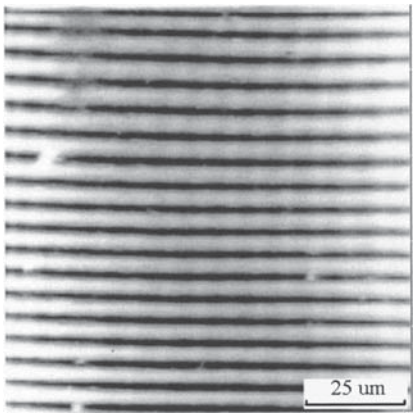

FIG. 7. Parallel moiré pattern at point O.

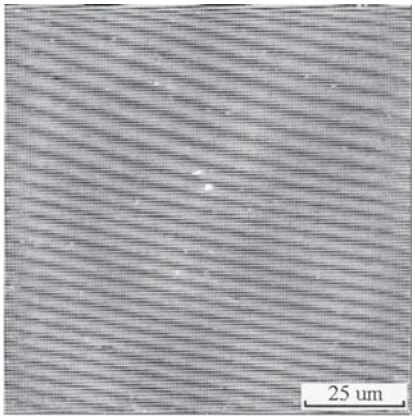

FIG. 9. *V*-field moiré fringes.

strain from the isothermal loading. The moiré fringes tend to be sparser away from the corner.

Figure 11 shows the shear strain distribution along the die corner. The shear strain decreases in a similar manner to that of the normal strain.

V. DISCUSSION

In this study, a Digital Instrument Dimension 3000 SPM equipped with a ''G'' scanner was utilized. This scanner has a typical maximum scan size of 90 μm. However, some piezomaterials were damaged and after replacement and recalibration, it can now scan a size as large as 109 μm. Then, a null field can be obtained when the scan size is 107 μm and the number of scanning lines is 128 for the 1200 lines/mm diffraction grating.

A. Calibration of scanner and measuring error

For any moiré technique, accuracy is always most important. Before this experiment, the scanner was calibrated using a VLSI standard sample (STR10-1800). This standard sample has a nominal error within 2%. Linearity and sensitivity were both finely calibrated for the *x* and *y* axes at 0° to ensure an error of less than 1%. Linearity calibration determines the uniformity of the reference grating; sensitivity calibration determines the pitch of the reference grating. Calibration parameters for scanner were adjusted while measured values were compared with known dimensions. However, due to several factors in the calibration work, such as resolution of display monitor, human error, plus the standard sample error, the lateral and vertical error can be as high as 3%.

In this study, the diffraction grating was taken as two parallel gratings orthogonal to each other, so both the *U*- and *V*-field moiré fringes can be recorded by switching the scan angle between 0° and 90°. Since the linearity of the *x* and *y* axes was only calibrated at 0°, the linearity at 90° was then examined before the measurements were carried out. It was found to be fairly good. However, later when the piezotube was replaced and recalibrated, the linearity was poor when the scan angle was changed to 90°. The linearity changed, probably because this G scanner was designed for topography measurement, so large sizes were seldom scanned at the 90° scan angle if it could be done at 0°. If the linearity was poor at 90°, then the only way to record both the *U*- and *V*-field moiré fringes in such cases was to rotate the sample 90° after the *U*- or *V*-field fringes were captured.

It is also well known that the scanner moves in a different manner between scanning downward and upward, and the linearity may change significantly if the slow axis direction changes. Because the SPM system used in this study was calibrated when scanning downward, all the moiré fringes above were captured in the same manner.

B. Advantage and adaptability of the AFM moiré technique

SPM can achieve a scan size in a range from several nanometers to 150 μm or more. Thus, the AFM moiré technique can observe very tiny deformation in the nanoscale as

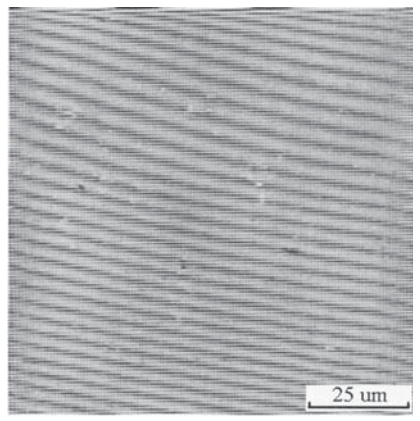

FIG. 8. *U*-field moiré fringes.

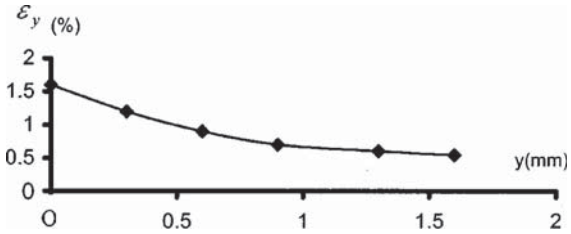

FIG. 10. Normal strain distribution along the *y* axis.

Reuse of AIP Publishing content is subject to the terms at: https://publishing.aip.org/authors/rights-and-permissions. Download to IP: 155.69.24.171 On: Sat, 03 Sep 2016 08:32:32

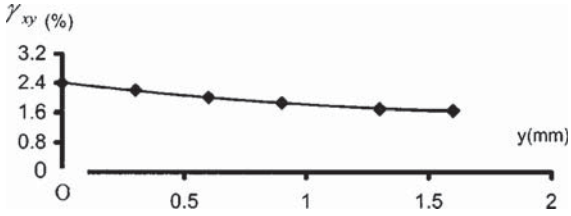

FIG. 11. Shear strain distribution along the y axis.

well as in the macroscale. Since the sensitivity of moiré techniques is determined by the specimen grating, the sensitivity can be greatly improved if a specimen grating of higher frequency is used. For the AFM used in this study, the scan size can be smaller than 1 μm. If 512 scan lines are used, the frequency of the specimen grating can reach as high as 512 000 lines/mm. Traditional moiré interferometers cannot use 3600 lines/mm specimen grating due to diffraction limitation. Thus, if a proper matching specimen grating is used, a much higher resolution can be achieved than that with the traditional optical moiré interferometer. However, in this study, the 1200 lines/mm specimen grating could only achieve a sensitivity of 0.833 μm per fringe order. Further experiments could be done with 2400, 3600, and 4800 lines/mm gratings.

The disadvantage of the AFM moiré method is the mismatch between the reference grating and the specimen grating if the scan size is not properly chosen. Usually, the scanning lines of the AFM have only several options, such as 64, 128, 256, and 512. For an image with better resolution, 256 lines are usually required. Using 256 scan lines, in this application, the pitch value of the reference grating is less than half that of the specimen grating even though the scan size goes up to 100 μm. This renders the moiré fringes very hard to form when the scan size is limited. In this study, hardly any moiré fringes were observed when the scan size was 80 μm or less. A 2400 lines/mm grating would be much better. Whereas for 512 scan lines, a 4800 lines/mm specimen grating would be preferred. However, the cost will be much greater.

C. AFM moiré fringes under different modes

All the moiré fringes shown above were captured while collecting height data information. However, when the AFM is working under other modes such as the lateral force mode, the scanning lines are formed in a similar manner, and better fringe patterns have been reported.[4] In this study, both height and friction data were captured to form moiré fringes, as shown in Fig. 12. It is interesting that under lateral force mode another group of moiré fringes emerge. Though it is possible that subtractive and additive moiré fringes could exist in the same picture, extensive studies proved that the new fringe group could be neither subtractive nor additive. Further work should be done to explain their appearance.

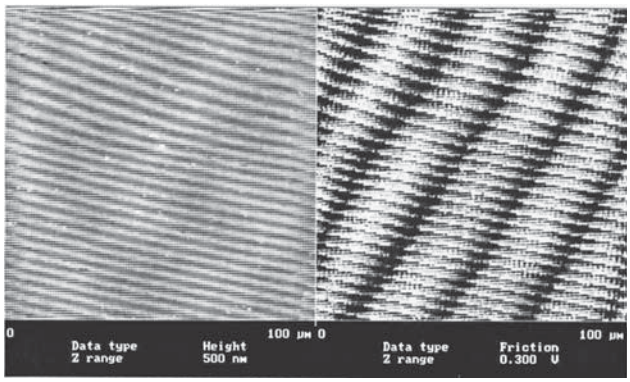

FIG. 12. Moiré fringes captured by collecting height and friction data (another group of fringes appears when collecting friction data).

ACKNOWLEDGMENT

The authors would like to express their sincere appreciation for the support from Nanyang Technological University.

[1] B. Han, Exp. Tech. **38**, 278 (1998).
[2] T. V. Vorburger, J. A. Dagata, G. Wilkening, and K. Lizuka, CIRP Ann. **46**, 597 (1997).
[3] H. Chen, D. Liu, and A. Lee, Exp. Tech. **24**, 31 (2000).
[4] H. Xie, S. Kishimoto, A. Asundi, G. B. Chai, N. Shinya, J. Yu, and B. K. A. Ngoi, Nanotechnology **11**, 24 (2000).
[5] Y. Morimoto and T. Hayashi, Exp. Mech. **24**, 112 (1984).
[6] Q. X. Cao, *Principle and Application of High-frequency Grating Moiré* (Tsinghua University, Beijing, 1983).

Reuse of AIP Publishing content is subject to the terms at: https://publishing.aip.org/authors/rights-and-permissions. Download to IP: 155.69.24.171 On: Sat, 03 Sep 2016 08:32:32